Long range transport of a quasi isolated chlorophyll patch by an Agulhas ring

Yoav Lehahn,[1,2] Francesco d'Ovidio,[3] Marina Lévy,[3] Yael Amitai,[4] and Eyal Heifetz[1]

Received 19 June 2011; revised 27 July 2011; accepted 27 July 2011; published 30 August 2011.

[1] Using satellite retrievals of sea surface chlorophyll and geostrophic currents we study the evolution of a distinct chlorophyll patch transported by an Agulhas ring along a ~1,500 km track. Throughout an ~11 months period of the total 2 years eddy lifetime, the shape of the chlorophyll patch is consistently delimited by the horizontal transport barriers associated with the eddy. Analysis of Lagrangian time series of sea surface variables in and around the eddy suggests that the evolution of the chlorophyll patch is driven by two processes (i) slow lateral mixing with ambient waters mediated by horizontal stirring in filaments, and (ii) rapid events of wind induced vertical mixing. These results support the idea that mesoscale eddies shape biological production through the combination of horizontal and vertical dynamical processes, and emphasize the important role of horizontal eddy transport in sustaining biological production over the otherwise nutrient-depleted subtropical gyres.
Citation: Lehahn, Y., F. d'Ovidio, M. Lévy, Y. Amitai, and E. Heifetz (2011), Long range transport of a quasi isolated chlorophyll patch by an Agulhas ring, *Geophys. Res. Lett.*, *38*, L16610, doi:10.1029/2011GL048588.

1. Introduction

[2] Mesoscale eddies play a fundamental role in the transport of material and dynamical quantities over different parts of the World Ocean [*Danabasoglu et al.*, 1994]. The importance of horizontal eddy transport is manifested at the Agulhas Current system, where Agulhas rings - the largest mesoscale eddies in the world Ocean [*Olson and Evans*, 1986] - are key agents in the transfer of warm and salty waters from the Indian Ocean to the South Atlantic [*Lutjeharms*, 2007]. Agulhas rings shed intermittently from the Agulhas retroflection south of Africa, have been shown to contribute to approximately 50% of the total heat and mass fluxes across the Aghulas Ridge [*Treguier et al.*, 2003].

[3] Agulhas rings travel across contrasted biogeochemical regimes, from relatively productive waters to the oligotrophic waters of the south Atlantic subtropical gyre. As suggested by conceptual and numerical model studies [*Lee and Williams*, 2000; *Oschlies*, 2002; *McGillicuddy et al.*, 2003; *Lévy*, 2003; M. Lévy et al., Large-scale impacts of submesoscale dynamics on phytoplankton: Local and remote effects, submitted to *Ocean Modelling*, 2011], horizontal eddy transport of nutrient rich waters across inter-regional routes may contribute significantly to the sustainment of primary production in the otherwise nutrient-depleted subtropical gyre. Despite its apparent importance, the biogeochemical consequence of long range transport by Agulhas rings lacks observational evidence.

[4] In this work we address this issue by analyzing the co-evolution of a chlorophyll (Chl) patch and the Agulhas ring within which it is bounded, using multi-satellite data. Most commonly, observations of Chl patches within eddies are attributed to vertical processes that lift nutrients into the well lit layer at the sea surface. Possible mechanisms include the uplift of nutrients through shoaling of density surfaces in cyclonic eddies [*McGillicuddy et al.*, 1998] and through wind induced Ekman upwelling in anticyclonic eddies [*Martin and Richards*, 2001; *McGillicuddy et al.*, 2007]. Here we show for this case evidence to other controls of mesoscale Chl patchiness, notably trapping of recycled nutrient through eddy isolation, coupled with modulation of the mixed layer through wind events.

2. Satellite Data

[5] Surface Chl and sea surface temperature (SST) are derived from the Moderate Resolution Imaging Spectroradiometer (MODIS) aboard Aqua. The dataset comprise of 4 km Level 3 images obtained from the ocean color data distribution site (http://oceandata.sci.gsfc.nasa.gov/). Since the ocean surface is often masked by clouds, the images are composed of satellite retrievals from 8 consecutive days.

[6] Geostrophic velocity field (GVF) is obtained from the AVISO database (http://www-aviso.cnes.fr). For the period of our study, the distributed global product combines altimetric data from the Envisat ERS, and Jason-1 mission. The data is gridded on a 1/3° × 1/3° Mercator grid, with one data file every seven days. The product also includes the MDT-05 mean dynamic topography [*Rio and Hernandez*, 2004]. Trajectories used for Lagrangian analysis were computed by integrating the geostrophic velocities with a Runge-Kutta scheme of the fourth order with a fixed time step of 6 hours.

3. Results and Discussion

[7] Marine eddies are commonly regarded as impermeable systems that trap particles for times comparable with the eddy's lifetime [*Provenzale*, 1999]. A useful way to characterize the isolated region at the eddy's core is calculating the Okubo-Weiss parameter (OW) [*Okubo*, 1970; *Weiss*, 1991], which is a measure of the relative dominance of vorticity (associated with the eddy's core, negative OW in Figure 1a)

[1]Department of Geophysics and Planetary Sciences, Tel Aviv University, Ramat Aviv, Israel.
[2]Department of Environmental Sciences, Weizmann Institute, Rehovot, Israel.
[3]Laboratoire d'Océanographie et du Climat: Expérimentation et Approches Numériques, IPSL, Université Pierre et Marie Curie, Paris, France.
[4]Earth Science institute, Hebrew University of Jerusalem, Jerusalem, Israel.

0094-8276/11/2011GL048588

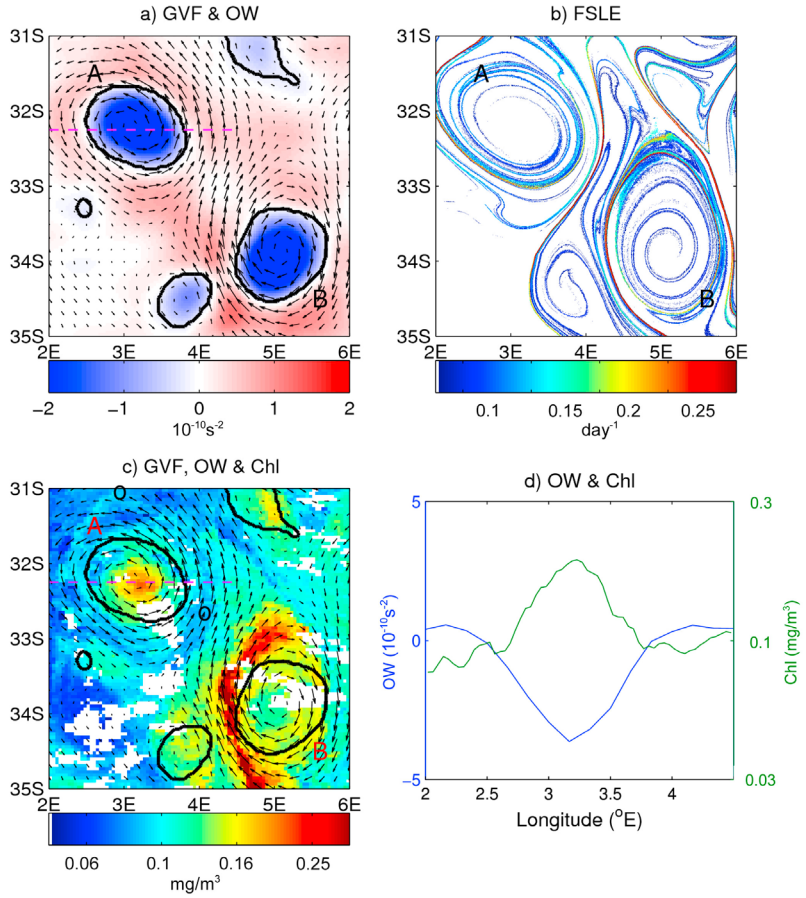

Figure 1. Two-dimensional images of (a) OW, (b) FSLE, and (c) Chl. The arrows and contours (Figures 1a and 1b) represent respectively the geostrophic surface currents and the 2×10^{-10} s^{-2} OW isoline, which marks the boundaries of eddy's core. (d) Cross-sections of OW (blue) and Chl (green) across the eddies diameter (dashed line in Figures 1a and 1c). The figures are from the 24 November 2006. All Chl images hereafter are composed of 8 consecutive days centered at the date provided in the text or in the title.

and deformation (associated with the eddy's periphery, positive OW in Figure 1a). Here we delimit the core boundaries by the 2×10^{-10} s^{-2} OW isoline (black contours in Figures 1a, 1c, 2, and 3).

[8] Recent studies based on dynamical systems tools, suggest however that the picture of marine eddies being impermeable to inward and outward fluxes of particle is an approximation, in principle only valid for eddies with no temporal variability [*Lehahn et al.*, 2007; *Beron-Vera et al.*, 2008, *d'Ovidio et al.*, 2009]. A measure of the extent to which a given eddy is sensitive to intrusion of ambient waters is provided by the structure of unstable manifolds (also referred to as attracting Lagrangian coherent structures [see *Haller and Yuan*, 2000]) from calculation of finite size Lyapunov exponents (FSLE) [*Boffetta et al.*, 2001; *d'Ovidio et al.*, 2004; *Lehahn et al.* 2007] (Figure 1b). These manifolds induce in advected tracer fields filament patterns with typical length in the range of ~10–~100 km and lifetime in the range of days/weeks (though it can be much longer if the patterns are associated to long-lived and energetic mesoscale features with low temporal variability). Since unstable manifolds represent transport barriers and tracer boundaries (see for example the strong unstable manifold enclosing the Chl filament at the periphery of eddy-B, Figures 1b and 1c, respectively), the more a given vortex is associated with spiraling unstable manifolds, the more it is subject to horizontal intrusion of ambient particles through horizontal stirring. Accordingly, since eddy B is associated with distinct spiraling unstable manifolds, it can be considered as relatively *permeable* to intrusion of ambient waters, while eddy A, whose core is encircled by the unstable manifolds, is likely to be *impermeable*. As a measure to the eddy's sensitivity to horizontal intrusion of ambient waters, we estimate the *eddy permeability* parameter, which is defined as the rate of change in the portion of particles trapped within the eddy's core (*eddy permeability* of a perfectly isolated eddy would be 0). A quantified view on the permeability of eddy-A to horizontal water intrusion (namely the *eddy permeability* parameter) is provided below. Note that in addition to the apparent difference in horizontal permeability, eddy-A and eddy-B are characterized by an opposite sense of rotation (anti-cyclonic and cyclonic, respectively), and hence differ in various dynamical and biological properties.

[9] The sensitivity of a given eddy to inward and outward horizontal flux of particles detected from the Lagrangian analysis of altimetry data has further confirmations in the biological field of surface Chlorophyll. Focusing on the *impermeable* eddy studied here (eddy-A), the physical-biological interplay takes the form of a pronounced circular Chl patch at the heart of the eddy (Figure 1c). The bound-

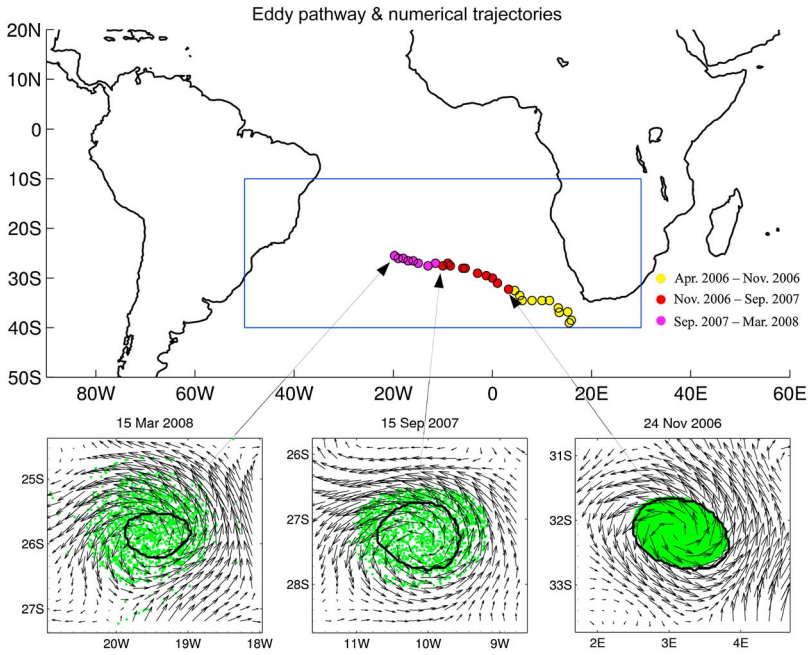

Figure 2. Background image: Pathway of eddy-A from the Agulhas retroflection to the heart of the south Atlantic subtropical gyre. Red circles represent the section where the core of the eddy is associated with a distinct Chl patch. Yellow and magenta circles mark the sections with no distinct Chl anomaly. The blue box delimits the extension of the background image in Figure 3. Subplots: Trajectories of synthetic numerical particles advected by the satellite derived velocity field (green dots), and the 2×10^{-10} s^{-2} OW isoline marking the boundaries of eddy's core (black contour).

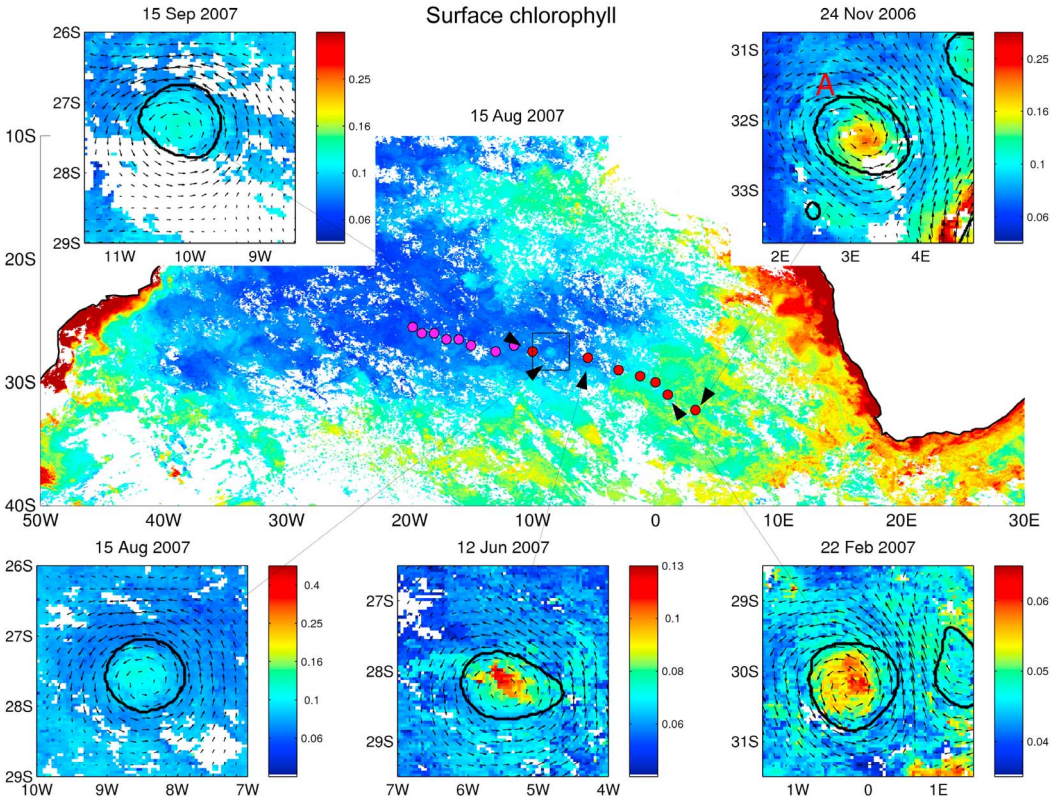

Figure 3. Background image: Surface chlorophyll in the Southern Atlantic on 15 August 2007. Red circles mark the section where the core of the eddy is associated with a distinct Chl patch (similarly to Figure 2). Subplots: Chl (colors), surface currents (arrows) and the 2×10^{-10} s^{-2} OW isoline marking the boundaries of the eddy's core (contour), at different times and locations along the eddy's track. Note differences in color scale (in order to emphasize the spatial structure of the Chl anomalies).

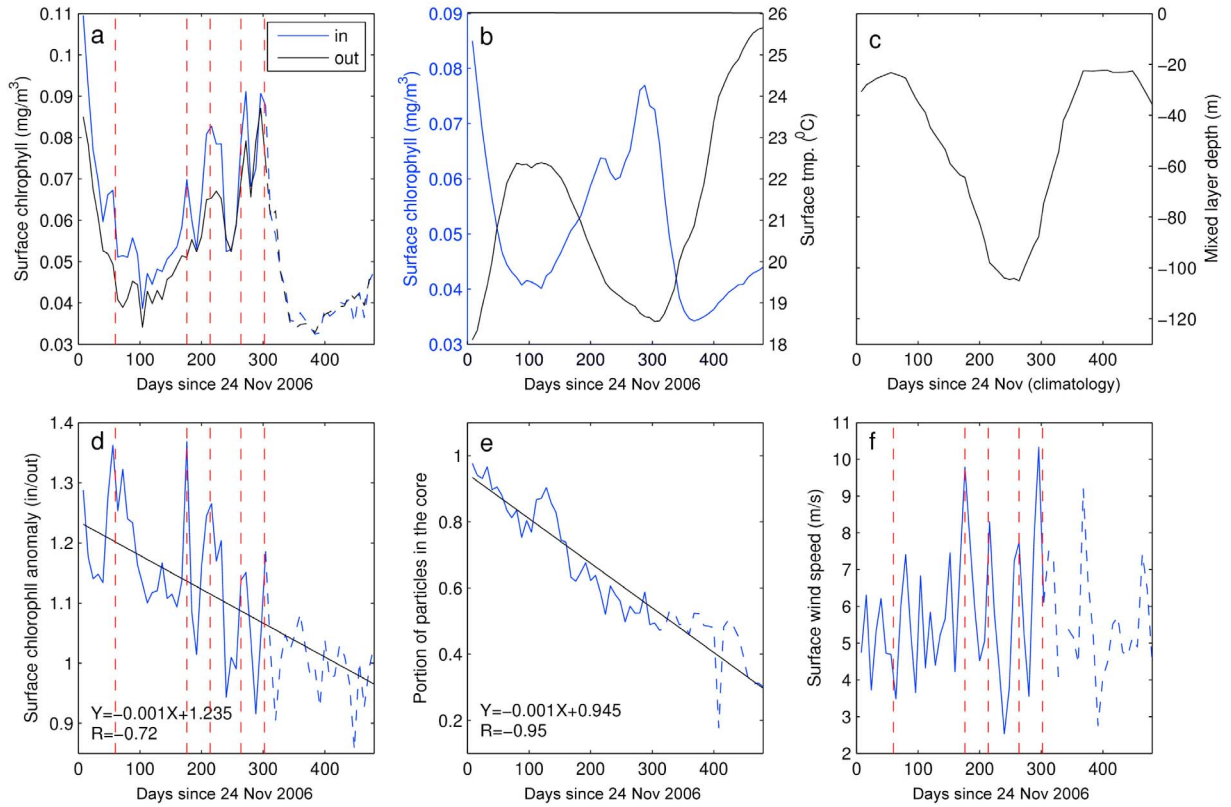

Figure 4. Lagrangian (i.e., varying in space according to the location of the eddy) time series of (a) Chl in (Chl_{in}, blue line) and around (Chl_{out}, black line) the eddy, (b) Chl (blue) and SST (black), (c) MLD climatology, (d) Chl anomaly (the ratio Chl_{in}/Chl_{out}), (e) Portion of particles trapped within the eddy's core, and (f) Surface wind speed (from QuikSCAT). For all fields, a given time step is composed of 8 consecutive days. In Figures 4b and 4c the signals are smoothed by a 5 step running window. The period characterized by a distinct Chl patch (red circles in Figure 2) and the period following that (magenta circles in Figure 2) are distinguished by solid and dashed lines, respectively. Vertical dashed lines mark the 5 main peaks in Chl anomalies (Figure 4d). Black lines in Figures 4d and 4e mark the linear regression fit.

aries of the patch clearly coincide with those of the eddy's core (identified by the 2×10^{-10} s^{-2} OW isoline described above), implying that the patch's extension is constrained by the eddy's dynamics and that indeed the core of the eddy is well isolated from its ambient waters. This is further emphasized when comparing cross-sections of Chl and OW along the patch's diameter, with both fields peaking simultaneously at the center of the eddy (Figure 1d).

[10] The Agulhas ring "Eddy-A" is a long-lived (~2 years, between April 2006 and March 2008) vortex traveling more than 4000 km, from the flanks of the Agulhas retroflection to the interior of the south Atlantic subtropical gyre (yellow, red and magenta circles in the background panel of Figure 2). Analysis of the eddy's transport properties is performed through a numerical experiment in which we compute the trajectories of synthetic particles initiated within the core of the eddy and advected by the satellite derived velocity field. The experiment is initiated on the 24 November 2006, when a distinct Chl patch at the eddy's core first spears (Figure 1c). The particles are initiated at the eddy's core (grid points associated with OW $< 2 \times 10^{-10}$ s^{-2}) and throughout the experiment their distribution is compared with the core's location and extension (small panels in Figure 2). Throughout the integration time (24 November 2006–15 March 2008, red and magenta circles in Figure 2) most particles remain aggregated in the vicinity of the eddy, while the number of particle actually trapped within the eddy's core decreases with time (and distance), reaching a low of ~30% (see Figure 4e).

[11] In partial accordance with the numerical experiment, throughout a period of ~11 months (November 2006–September 2007, red circles in Figures 2 and 3), during which the eddy traveled approximately 1500 km, the core of the eddy was associated with a distinct Chl patch. Similarly to the picture in day one of the analysis (24 November 2006, Figure 1c), throughout this period the shape of the patch is delimited by the boundaries of the eddy's core (see for instance the small panels in Figure 3). Along this part of the eddy's track Chl concentrations at the core of the eddy were consistently higher than those in the surrounding waters. During other periods of the eddy lifetime (yellow and magenta circles in Figure 2) the patch is absent and Chl concentrations within the core of the eddy are similar to those in the surrounding waters.

[12] The distribution patterns of synthetic particles in the vicinity of the eddy, together with the consistent similarity between the eddy's morphology and the structure of the Chl patch, confirms that eddy-A acts as a *quasi isolated system* that is separated from its surroundings by transport barriers induced by horizontal stirring. Accordingly, we define a *quasi isolated eddy* as a vortex for which the residence time of its content is comparable (same order of magnitude) to

the lifetime of the eddy itself. As such, the eddy traps remineralized nutrients, thus sustaining relatively high rates of primary production (as expressed by the positive Chl anomalies) over a period of several months.

[13] Analysis of patch's evolution is done through extraction of Lagrangian (i.e., varying in space according to the location of the eddy) time series of different parameters, at the eddy's core and over a 4 × 4° region around the eddy (Figure 4). Overall, Chl within the eddy's core (Chl_{in}, blue line in Figure 4a) shows a similar evolution pattern as that of Chl in the waters surrounding the eddy (Chl_{out}, black line in Figure 4a). Comparison between smoothed signals of Chl and sea surface temperature (SST, blue and black lines in Figure 4b, respectively) suggests that both in and around the eddy, the low frequency Chl signal is driven primarily by change in mixed layer depth (MLD). According to this scenario, which is typical to subtropical gyres where phytoplankton growth is mainly limited by the availability of nutrients [*Lévy et al.*, 2005], Chl concentrations increase (decrease) with the deepening (shallowing) of the mixed layer, as manifested in the SST field. This scenario is supported by the Lagrangian evolution of MLD climatology from *de Boyer-Montégut et al.* [2004], showing similar seasonal pattern as that of SST (Figure 4c).

[14] The temporal change in the intensity of the Chl anomaly (defined as the ratio Chl_{in}/Chl_{out}, Figure 4d), is characterized by high frequency fluctuations (main peaks marked by red dashed lines in Figures 4a, 4d, and 4f) that are superimposed on a monotonous decrease. Based on the suggested above scenario of eddy-A being a quasi isolated nutrient-rich system, this evolution pattern can be interpreted as resulting from two processes, acting on different time-scales:

[15] 1. Exchange of waters between the eddy and its surroundings, resulting in a progressive decrease of the total pool of organic and inorganic material trapped in the eddy's core (and thus a weaker Chl signature). To measure the importance of this effect, we estimate the described above *eddy permeability* parameter, by calculating the change rate of the portion of synthetic particles remaining within the eddy's core (i.e., particles associated with $OW < 2 \times 10^{-10}\ s^{-2}$) (Figure 4e). Here, the trend expressed by the *eddy permeability* parameter (i.e., the slope of the regression line in Figure 4e) is remarkably similar to the rate of weakening in the patch's intensity (i.e., the slope of the regression line in Figure 4d). The rate of particle loss is in agreement with results from a model study of *de Steur et al.*, [2004], showing that during the first months of an Agulhas ring lifetime, 40% of its thermocline waters is mixed away.

[16] 2. Strong wind events (Figure 4f, note the collocation of the peaks in patch intensity and in surface wind speeds) that induce high frequency increase of Chl_{in} and Chl_{out} through enhancement of vertical mixing and, consequently, entrainment of nutrients into the photic layer. The Chl increase is systematically larger inside the eddy than outside (Figure 4d), which suggests that the wind-induced nutrient supply is enhanced inside the eddy. We hypothesize that the larger wind-induced nutrient supply in the eddy results from a larger sub-surface nutrient pool within the eddy. This is consistent with the eddy originating from a nutrient rich area, embodying a column a water that extends well below the euphotic layer (typically 500 m) and progressing in the subtropical gyre where the nutricline is depressed. Alternatively, strong wind events may enhance Chl_{in} through the eddy/wind interaction mechanism whereby the eddy's circulation interacts with a spatially uniform wind field to induce Ekman pumping of nutrient rich waters at the eddy' s core [*Martin and Richards*, 2001; *McGillicuddy et al.*, 2007]. Production from submesoscale processes at the eddy's periphery (even if possibly followed by accumulation at the eddy's center [e.g., *Mahadevan et al.*, 2008]) is a less likely scenario, since Chl consistently peaks at the eddy's centroid (Figure 3). Note moreover that since eddy-A is an anticyclone, the elevated Chl values in its core cannot result from the well-known eddy pumping mechanism [*McGillicuddy et al.*, 1998].

[17] The consistent similarity between the eddy's transport structure and the shape of the Chl patch suggests that the Agulhas ring "eddy-A" is a *quasi-isolated system* that transport nutrient-rich waters between remote oceanographic regions. This can be regarded as a specific case of a "dynamical phytoplankton niche" [*d'Ovidio et al.*, 2010], characterized by elevated production rates enabled by in-situ remineralization of the initial nutrient pool. These results support the idea that mesoscale eddies shape biological production through combination of horizontal and vertical dynamical processes [*Williams and Follows*, 2003], and emphasizes the important role of horizontal eddy transport in sustaining biological production over the nutrient-depleted subtropical gyres [*Lee and Williams*, 2000; *Oschlies*, 2002; *Lévy*, 2003].

[18] **Acknowledgments.** The authors acknowledge support from the ANR SOUTHERNCROSS. NASA for access to MODIS L3 data. The altimeter products were produced by Ssalto/Duacs and distributed by Aviso with support from the Centre National d'Études Spatiales. QuikScat data are produced by Remote Sensing Systems and sponsored by the NASA Ocean Vector Winds Science Team. Data are available at www.remss.com.

[19] The Editor thanks two anonymous reviewers for their assistance in evaluating this paper.

References

Beron-Vera, F., M. Olascoaga, and G. Goni (2008), Oceanic mesoscale eddies as revealed by Lagrangian coherent structures, *Geophys. Res. Lett.*, *35*, L12603, doi:10.1029/2008GL033957.

Boffetta, G., G. Lacorata, G. Redaelli, and A. Vulpiani (2001), Detecting barriers to transport: A review of different techniques, *Physica D*, *159*, 58–70, doi:10.1016/S0167-2789(01)00330-X.

Danabasoglu, G., J. McWilliams, and P. R. Gent (1994), The role of mesoscale tracer transport in the global ocean circulation, *Science*, *264*, 1123–1126, doi:10.1126/science.264.5162.1123.

de Boyer-Montégut, C., G. Madec, A. S. Fischer, A. Lazar, and D. Iudicone (2004), Mixed layer depth over the global ocean: An examination of profile data and a profile based climatology, *J. Geophys. Res.*, *109*, C12003, doi:10.1029/2004JC002378.

d'Ovidio, F., V. Fernández, E. Hernández-Garcıá, and C. López (2004), Mixing structures in the Mediterranean Sea from finite-size Lyapunov exponents, *Geophys. Res. Lett.*, *31*, L17203, doi:10.1029/2004GL020328.

d'Ovidio, F., J. Isern-Fontanet, C. López, E. García-Ladona, and E. Hernández-García (2009), Comparison between Eulerian diagnostics and the finite-size Lyapunov exponent computed from altimetry in the Algerian Basin, *Deep Sea Res., Part I*, *56*, 15–31, doi:10.1016/j.dsr.2008.07.014.

d'Ovidio, F., S. De Monte, S. Alvain, Y. Dandonneau, and M. Lévy (2010), Fluid dynamical niches of phytoplankton types, *Proc. Natl. Acad. Sci. U. S. A.*, *107*, 18,366–18,370, doi:10.1073/pnas.1004620107.

de Steur, L., P. van Leeuwen, and S. Drijfhout (2004), Tracer leakage from modeled Agulhas rings, *J. Phys. Oceanogr.*, *34*, 1387–1399, doi:10.1175/1520-0485(2004)034<1387:TLFMAR>2.0.CO;2.

Haller, G., and G. Yuan (2000), Lagrangian coherent structures and mixing in two-dimensional turbulence, *Physica D*, *147*, 352–370, doi:10.1016/S0167-2789(00)00142-1.

Lee, M., and R. Williams (2000), The role of eddies in the isopycnic transfer of nutrients and their impact on biological production, *J. Mar. Res.*, *58*, 895–917, doi:10.1357/002224000763485746.

Lehahn, Y., F. d'Ovidio, M. Lévy, and E. Heifetz (2007), Stirring of the northeast Atlantic spring bloom: A Lagrangian analysis based on multisatellite data, *J. Geophys. Res.*, *112*, C08005, doi:10.1029/2006JC003927.

Lévy, M. (2003), Mesoscale variability of phytoplankton and of new production: Impact of the large-scale nutrient distribution, *J. Geophys. Res.*, *108*(C11), 3358, doi:10.1029/2002JC001577.

Lévy, M., Y. Lehahn, J.-M. André, L. Mémery, H. Loisel, and E. Heifetz (2005), Production regimes in the northeast Atlantic: A study based on SeaWiFS chlorophyll and ocean general circulation model mixed layer depth, *J. Geophys. Res.*, *110*, C07S10, doi:10.1029/2004JC002771.

Lutjeharms, J. (2007), Three decades of research on the greater Agulhas Current, *Ocean Sci.*, *3*, 129–147, doi:10.5194/os-3-129-2007.

Mahadevan, A., L. N. Thomas, and A. Tandon (2008), Comment on "Eddy/wind interactions stimulate extraordinary mid-ocean plankton blooms", *Science*, *320*, 448, doi:10.1126/science.1152111.

Martin, A., and K. Richards (2001), Mechanisms for vertical nutrient transport within a North Atlantic mesoscale eddy, *Deep Sea Res., Part II*, *48*, 757–773, doi:10.1016/S0967-0645(00)00096-5.

McGillicuddy, D. J., A. R. Robinson, D. A. Siegal, H. W. Jannasch, R. Johnson, T. D. Dicky, J. Mcneil, A. F. Michaels, and A. H. Knap (1998), Influence of mesoscale eddies on new production in the Sargasso Sea, *Nature*, *394*, 263–266, doi:10.1038/28367.

McGillicuddy, D. J., Jr., L. A. Anderson, S. C. Doney, and M. E. Maltrud (2003), Eddy-driven sources and sinks of nutrients in the upper ocean: Results from a 0.1° resolution model of the North Atlantic, *Global Biogeochem. Cycles*, *17*(2), 1035, doi:10.1029/2002GB001987.

McGillicuddy, D., et al. (2007), Eddy/wind interactions stimulate extraordinary mid-ocean plankton blooms, *Science*, *316*, 1021–1026, doi:10.1126/science.1136256.

Okubo, A. (1970), Horizontal dispersion of floatable particles in the vicinity of velocity singularities such as convergences, *Deep Sea Res. Oceanogr. Abstr.*, *17*, 445–454, doi:10.1016/0011-7471(70)90059-8.

Olson, D., and R. Evans (1986), Rings of the Agulhas Current, *Deep Sea Res., Part A*, *33*, 27–42, doi:10.1016/0198-0149(86)90106-8.

Oschlies, A. (2002), Nutrient supply to the surface waters of the North Atlantic: A model study, *J. Geophys. Res.*, *107*(C5), 3046, doi:10.1029/2000JC000275.

Provenzale, A. (1999), Transport by coherent barotropic vortices, *Annu. Rev. Fluid Mech.*, *31*, 55–93, doi:10.1146/annurev.fluid.31.1.55.

Rio, M.-H., and F. Hernandez (2004), A mean dynamic topography computed over the world ocean from altimetry, in situ measurements, and a geoid model, *J. Geophys. Res.*, *109*, C12032, doi:10.1029/2003JC002226.

Treguier, A., O. Boebelb, B. Barnier, and G. Madec (2003), Agulhas eddy fluxes in a 1/6 Atlantic model, *Deep Sea Res., Part II*, *50*, 251–280, doi:10.1016/S0967-0645(02)00396-X.

Weiss, J. (1991), The dynamics of enstrophy transfer in two-dimensional hydrodynamics, *Physica D*, *48*, 273–294, doi:10.1016/0167-2789(91)90088-Q.

Williams, R., and M. Follows (2003), Physical transport of nutrients and the maintenance of biological production, in *Ocean Biogeochemistry: The Role of the Ocean Carbon Cycle in Global Change*, edited by M. J. R. Fasham, pp. 19–51, Springer, Berlin.

Y. Amitai, Earth Science institute, Hebrew University of Jerusalem, Jerusalem 91904, Israel. (yaela70@gmail.com)

F. d'Ovidio and M. Lévy, Laboratoire d'Océanographie et du Climat: Expérimentation et Approches Numériques, IPSL, Université Pierre et Marie Curie, BC 100, 4 place Jussieu, F-75005 Paris CEDEX, France. (francesco.dovidio@locean-ipsl.upmc.fr; marina@locean-ipsl.upmc.fr)

E. Heifetz, Department of Geophysics and Planetary Sciences, Tel Aviv University, Ramat Aviv 69978, Israel. (eyalh@post.tau.ac.il)

Y. Lehahn, Department of Environmental Sciences, Weizmann Institute, Rehovot 76100, Israel. (yoav.lehahn@weizmann.ac.il)